Skeletal Relaxation Effect on the Charge Transfer State Formation of 4-Dimethylamino,4′-cyanostilbene

Yoshiaki Amatatsu*

Faculty of Engineering and Resource Science, Akita University, Tegata Gakuen-cho, Akita 010-8502, Japan

Received: March 2, 2006; In Final Form: May 9, 2006

Ab initio complete active space self-consistent field (CASSCF) calculations combined with polarized continuum model (PCM) have been performed to examine the charge transfer (CT) state formation of *trans*-4-dimethylamino,4′-cyanostilbene (DCS) in a solvent. In a polar solvent, the globally stable geometry in S_1 takes a twisted conformation where the electron-donating dimethylanilino group is highly twisted against the other part of the electron-withdrawing 4-cyanostyryl group. In addition, skeletal relaxation where the aromatic benzene rings turn to be a nonaromatic quinoid structure is essential to stabilize the CT state. In a nonpolar solvent, the stable geometry in S_1 takes a nontwisted conformation, though the skeletal relaxation is also an essential factor. By means of the free energy decomposition analysis, it is found that the stable CT geometry which depends on solvent polarity mainly comes from two factors: the linkage bond between the dimethylanilino and the 4-cyanostyryl group and the electrostatic interaction. In a polar solvent, the linkage bond has a single bond character to slightly prevent the torsional motion. This twist geometrically assists the charge separation so as to reinforce the electrostatic interaction. In consequence, the twisted internal CT (TICT) conformation is stable. In a nonpolar solvent, on the other hand, a nontwisted CT state is stable because the linkage bonds greatly increase a double bond character so as to prevent the torsional motion, while the electrostatic interaction is not so enhanced even by the geometrical twist.

1. Introduction

The formation of the photoinduced charge transfer (CT) state of the push−pull π-conjugated molecule is one of the most important processes in photochemistry. The main concern is what the geometry of the CT state is. As a typical example, the CT geometry of 4-dimethylaminobenzonitrile (DMABN) has been of great interest from both experiment and theory.[1] A most promising candidate for the CT geometry has been the twisted internal CT (TICT) geometry where the dimethylamino group is perpendicularly twisted against the remaining part.[2] This is because the geometrical twist serves to accomplish the charge separation between the electron-donating group and the electron-withdrawing group. However, we recently proposed that another factor of the skeletal relaxation (i.e., transformation from the aromatic benzene into the nonaromatic quinoid structure) is also important to stabilize the TICT state.[1] Our new model is, in a sense, a proper incorporation of a conventional TICT model with another PICT (planar internal CT) model. In the present study, we examine if both factors of geometrical twist and skeletal relaxation are important for the CT formation in another π-conjugated system of *trans*-4-dimethylamino,4′-cyanostilbene (DCS) in a solvent (see Figure 1).

In the following, we make a brief review on the photochemistry of DCS in a solvent. The photochemical behavior of DCS, which is strongly dependent on solvent polarity, has been also extensively studied from experiment.[3−12] In nonpolar cyclohexane, only one emitting state with a lifetime of 85 ps exists at 440 nm. In polar dimethylsolfoxide (DMSO), on the other hand, two types of red-shifted emitting states exist at 490 and 560 nm, respectively.[10] Therein it is observed that there is a precursor−successor relationship between the two emitting states. As the former emission with a lifetime of 4.5 ps decays, the latter one with a much longer lifetime of 920 ps emerges. To confirm what the geometry for the red-shifted emission is, the photochemical behaviors of several DCS derivatives were examined. In case of the rigidified *p*-dimethylamino,*p*″-cyano,1-

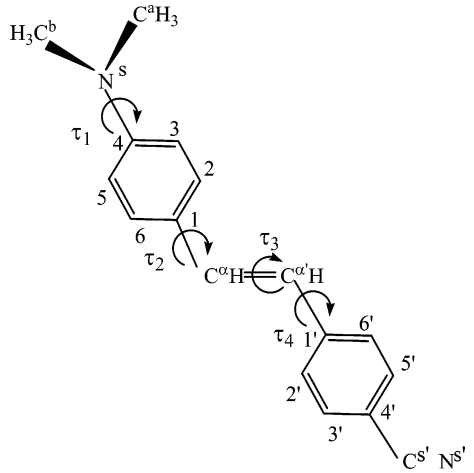

Figure 1. Numberings of atoms of the DCS skeleton. The torsional degrees of freedom τ_2, τ_3, and τ_4 are defined by the dihedral angles, $<C^2C^1C^\alpha C^{\alpha'}$, $<C^1C^\alpha C^{\alpha'}C^{1'}$, and $<C^\alpha C^{\alpha'}C^{1'}C^{2'}$, respectively. τ_1 is defined by the dihedral angle between the two planes of which normal vectors are $\{\mathbf{r}(C^4C^5) \times \mathbf{r}(C^4C^3)\} \times \mathbf{r}(C^4N^s)$ and $\{\mathbf{r}(N^sC^a) \times \mathbf{r}(N^sC^b)\} \times \mathbf{r}(N^sC^4)$. DCS is divided into three fragments: **A**, dimethyanilino group $(CH_3)_2N-C_6H_4-$; **B**, ethylenic part $-C^\alpha H{=}C^{\alpha'}H-$; and **C**, benzonitrile group $-C_6H_4CN$.

* Corresponding author phone: +81-18-889-2625; fax: +81-18-889-2601; e-mail: amatatsu@ipc.akita-u.ac.jp.

10.1021/jp061310s CCC: $33.50
Published on Web 06/23/2006

1′-bi-indanylidene which is prevented from both τ_2- and τ_4-torsional motions defined in Figure 1, the more red-shifted emission around 560 nm is not observed irrespective of solvent polarity.[5,10,11] On the other hand, two types of emissions similar to that of DCS are observed in another rigidified (3-*p*-dimethylanilino,7-cyano,1,2-dihydro)-naphthalene which is bridged by a six-membered ring between the ethylenic portion and the benzonitrile group to hinder the τ_3- and τ_4-torsional motion.[5,10] Also two types of red-shifted emissions are observed in another rigidified (3-(5′-*N*-methylindolinyl), 7-cyano,1,2-dihydro)-naphthalene which is prevented from τ_1-, τ_3- and τ_4-torsional motions.[5] From a theoretical side, we examined the potential energy surfaces with respect to the four torsional angles τ_i's (refer to Figure 1) so as to give a reasonable interpretation on the experimental findings mentioned above.[13,14] That is, the nontwisted CT state forms very fast after electronic excitation, and then the nontwisted CT changes into the TICT state by the dimethylanilino (i.e., τ_2) torsional motion in a polar solvent. To the best of our knowledge, however, there are no experimental and theoretical realizations that an additional factor is important for the CT formation process in a solvent besides the torsional motion of the dimethylanilino group and solvent polarity. In the present study, we examined the skeletal relaxation effect on the CT formation of DCS in a solvent by means of a reliable ab initio complete active space self-consistent field (CASSCF) calculation combined with polarized continuum model (PCM).

2. Method of Calculation

In the present calculations with the GAMESS program,[15] we reduced computational labor based on the results of our previous CASSCF calculations.[14] The active space was taken into account of the highest four occupied and the lowest four unoccupied orbitals (denoted by (8,8)CASSCF). This is because the present interest of S_1 with respect to the τ_2-torsional coordinate is well described by the configuration state functions within the excitations between the highest four occupied and the lowest four unoccupied orbitals. The diffuse orbital basis set, which was put on the ethylenic carbons in the previous calculation, was found to be less important for the present interest and the ethylenic carbons were removed. So we used a little smaller basis set: the Huzinage−Dunning double-ζ basis set augmented by polarization functions on the N atoms (α_d=0.80) and the central ethylenic C atoms (α_d=0.75) to ensure the flexibility of orbitals derived from them. In the free energy evaluation by means of (8,8)CASSCF calculation with PCM, we took into account only the electrostatic interaction as the interactions between DCS and a solvent. In general, the free energy can be expressed by summation of the internal energy in a solvent, electrostatic interaction, dispersion and repulsion energies, and cavitation energy which is intrinsic within a framework of PCM. However, as shown previously,[13] the cavitation, dispersion, and repulsion terms are not so changed as far as the τ_2-torsional motion is concerned. The constancy of these terms can be understood as follows. The dispersion and repulsion as well as the cavitation are mainly due to the contacts between the solute DCS and a solvent. So they are affected by a cavity shape of the solute within a framework of PCM. It was found that the shape and volume of the cavity are not so changed during the τ_2-torsional motion, although they are strongly dependent on the τ_3 torsional motion which relates to the cis−trans photoisomerization process. In addition, it was found in our experience that the evaluations of the dispersion and repulsion terms are much more time-consuming steps than those of the internal energy and electrostatic interaction. Therefore, we express the free energy $F_i(\tau_2)$ for a state i by eq 1

$$F_i(\tau_2) = E_i^{\mathrm{int}}(\tau_2) + E_i^{\mathrm{ES}}(\tau_2) \quad (1)$$

where $E_i^{\mathrm{int}}(\tau_2)$ and $E_i^{\mathrm{ES}}(\tau_2)$ are the internal energy and the electrostatic interaction for a state i at τ_2.

In the present calculations, we took the following steps. First, we optimized the geometry of S_0 in a polar solvent of DMSO (S_0/DMSO) and the globally stable geometry of S_1 in DMSO (S_1/DMSO). We then performed similar optimizations in a nonpolar solvent of cyclohexane (similarly denoted by S_0/CHEX and S_1/CHEX, respectively). To examine the solvent effect on the stable geometry in S_0, we performed an additional optimization of a bare DCS molecule in S_0 (S_0-bare) by means of (8,8)-CASSCF without PCM. Then we evaluated two types of free energy curves in S_1 with respect to τ_2, where τ_2 changes from 0° to 90° but the other geometrical parameters are fixed to those of S_0/DMSO, S_1/DMSO, S_0/CHEX, and S_1/CHEX, respectively. To check the validity of the present model by means of CASSCF, we performed the second-order multireference Möller−Plesset perturbation (MRMP2) calculations at several important conformations.

TABLE 1: Characteristic Optimized Parameters of DCS

	S_0-bare	S_0/CHEX	S_0/DMSO	S_1/CHEX	S_1/DMSO
			Bond Distances (Å)		
$C^{\alpha}C^{\alpha'}$	1.331	1.331	1.331	1.447	1.374
$C^{1}C^{\alpha}$	1.478	1.478	1.478	1.394	1.487
$C^{1'}C^{\alpha'}$	1.478	1.478	1.478	1.414	1.411
$C^{1}C^{2}$	1.413	1.414	1.414	1.456	1.442
$C^{2}C^{3}$	1.391	1.391	1.390	1.378	1.367
$C^{3}C^{4}$	1.424	1.424	1.424	1.452	1.447
$C^{4}C^{5}$	1.395	1.395	1.394	1.451	1.450
$C^{5}C^{6}$	1.401	1.402	1.402	1.356	1.392
$C^{6}C^{1}$	1.400	1.400	1.399	1.461	1.425
$C^{1'}C^{2'}$	1.412	1.412	1.418	1.452	1.432
$C^{2'}C^{3'}$	1.397	1.397	1.393	1.377	1.377
$C^{3'}C^{4'}$	1.406	1.405	1.410	1.426	1.401
$C^{4'}C^{5'}$	1.405	1.405	1.400	1.410	1.439
$C^{5'}C^{6'}$	1.385	1.385	1.398	1.376	1.366
$C^{6'}C^{1'}$	1.406	1.407	1.394	1.432	1.450
$N^{s}C^{4}$	1.408	1.409	1.411	1.336	1.340
$N^{s}C^{a}$	1.463	1.464	1.465	1.467	1.469
$N^{s}C^{b}$	1.460	1.460	1.461	1.467	1.469
$C^{4'}C^{s'}$	1.446	1.445	1.446	1.423	1.415
$C^{s'}N^{s'}$	1.140	1.139	1.137	1.142	1.135
			Torsional Angles (deg)		
τ_1	−3.2	−5.3	−7.6	−0.4	−4.3
τ_2	−0.0	−0.4	−0.0	0.9	90.0
τ_3	180.0	179.9	179.5	−178.3	179.7
τ_4	−0.0	−0.5	−0.4	1.3	−0.8
			Wagging Angle (deg)[a]		
ω	34.9	36.1	38.0	0.1	0.3

[a] The wagging angle ω is calculated by the inner product between $\mathbf{r}(C^4N^s)$ and the bisector vector of $< C^aN^sC^b$.

3. Results

3-1. S_1 Geometry in Cyclohexane. In Table 1, we listed the characteristic optimized parameters. The geometries of S_0/CHEX as well as S_0/DMSO are found to be similar to S_0-bare. This means that the stable structure in S_0 is not so affected by a solvent. The $C^{\alpha}C^{\alpha'}$ bond distance is a typical C=C double bond, and the CC bonds in the benzene rings are similar to that of the aromatic benzene ring. The N^sC^4 bond is somewhat shorter than a normal N−C single bond, which is ascribed to resonance between the dimethylamino group and the adjacent benzene ring.

TABLE 2: Dipole Moments and Mulliken Charges on Each Fragment

					Mulliken charge		
geometry	state	τ_2	solvent	dipole moment[a])	A	B	C
S_0-bare	S_0	−0.0	none	7.19	0.13	−0.16	0.03
S_0-bare	S_1	−0.0	none	18.41	0.42	−0.22	−0.20
S_0/CHEX	S_0	−0.4	cyclohexane	7.39	0.13	−0.16	0.03
S_0/CHEX	S_1	−0.4	cyclohexane	21.60	0.51	−0.23	−0.28
S_0/CHEX	S_1	−0.4	none	19.44	0.47	−0.24	−0.23
S_1/CHEX	S_1	0.9	cyclohexane	27.63	0.60	−0.23	−0.37
S_0/DMSO	S_0	−0.0	DMSO	7.43	0.12	−0.16	0.04
S_0/DMSO	S_1	−0.0	DMSO	30.52	0.68	−0.16	−0.52
S_0/DMSO	S_1	−0.0	cyclohexane	21.82	0.49	−0.20	−0.29
S_0(90)/DMSO[b])	S_1	90.0	cyclohexane	33.70	0.76	−0.21	−0.55
S_0(90)/DMSO	S_1	90.0	DMSO	36.08	0.80	−0.19	−0.61
S_1/DMSO	S_1	90.0	DMSO	38.27	0.81	−0.31	−0.50
S_1/DMSO	S_1	90.0	cyclohexane	35.93	0.78	−0.32	−0.46
S_1(0)/DMSO[c])	S_1	0.0	DMSO	30.08	0.65	−0.28	−0.37

[a] Units are given in Debye. [b] The geometry of S_0(90)/DMSO is obtained by $\tau_2 = 90°$, but the other parameters are fixed to those at S_0/DMSO. [c] The geometry of S_1(0)/DMSO is obtained by $\tau_2 = 0°$, but the other parameters are fixed to those at S_1/DMSO.

A similar feature is found in the $C^{4'}C^{s'}$ bond due to the resonance between the cyano group and the adjacent benzene ring. On the other hand, the resonance among the ethylenic part and the benzene rings is relatively small so that the linkage bonds of C^1C^α and $C^{\alpha'}C^{1'}$ almost hold a normal C−C single bond character. From the four torsional angles of τ_i's, DCS is found to keep a *trans*-form in S_0 substantially. The wagging angle is $\omega = 36.1°$ so that the dimethylamino group takes a nonplanar structure against the remaining stilbene skeleton. On the other hand, the stable geometry in S_1 strongly depends on solvent polarity. Regarding the S_1 stable geometry in a typical nonpolar solvent of cyclohexane (i.e., S_1/CHEX), the torsional angle τ_2 as well as the other three τ_i's (i=1,3,4) are not so different from those of S_0/CHEX. In other words, the stable S_1 geometry in cyclohexane takes a nontwisted conformation. However, the skeletal bond distances as well as the wagging angle ω are very different from those of S_0/CHEX. The aromatic benzene ring of the dimethylanilino group turns to be a nonaromatic quinoid structure: the C^2C^3 and C^5C^6 bonds shrink into a normal C=C double bond, while the C^1C^2, C^3C,[4] C^4C^5, and C^6C^1 bonds become longer. The other aromatic benzene ring of the benzonitrile part also turns to be a quinoid structure. The ethylenic $C^\alpha C^{\alpha'}$ bond elongates, while the linkage bonds of C^1C^α, $C^{\alpha'}C^{1'}$, and $C^{4'}C^{s'}$ become shorter. The N^sC^4 bond shrinks drastically, and the wagging angle ω is 0.1° so that the dimethyamino part takes a planar structure. This means that the dimethylamino part becomes much more resonant with the adjacent benzene ring. On the basis of the above computational findings, the skeletal relaxation, which leads to bond alternation of the π-conjugated system over the whole DCS skeleton, is an important factor to stabilize DCS in S_1 in a nonpolar solvent of cyclohexane.

Next we discuss the electronic structure in relation with the geometrical feature of S_1/CHEX mentioned above. As seen in Table 2, the dipole moments in S_1 take a large value irrespective of conformations so that DCS in S_1 has a CT character. In addition, it is found that the dipole moment in S_1 at S_0-bare (i.e., without a solvent) also takes a large value. This means that the CT character is intrinsic in S_1 of DCS itself. However, we also find out the dipole moment in the CT state depends on the conformation and solvent polarity. The dipole moment of S_1 at S_0/CHEX (21.60 D) is somewhat larger than that at the same conformation without a solvent (19.44 D). In other words, the surrounding solvent more polarizes DCS in S_1. Furthermore, the S_1 dipole moment at S_1/CHEX (27.63 D) is larger than that at S_0/CHEX (21.60 D) in cyclohexane. This is ascribed to another effect: the skeletal relaxation, where the aromaticity of the benzene rings disappears and the bond alternation over the whole π-conjugated system of DCS stabilizes the CT state in S_1. In consequence, the stable S_1 geometry in cyclohexane (i.e., S_1/CHEX) is a CT state of which geometry takes a nontwisted but skeletal-relaxed conformation. The analysis of Mulliken charge in each fragment gives more detailed insight of the CT character mentioned above. In comparison of Mulliken charges in S_1 with those in S_0 at S_0-bare, the electron is transferred from the dimethylanilino (i.e., fragment **A** defined in Figure 1) into the 4-cyanostyryl part (i.e., fragments **B**+**C**). That is, the dimethylanilino and the 4-cyanostyryl parts play roles of electron-donating and electron-withdrawing groups, respectively. In cyclohexane, the electron is more transferred from **A** to **C**, while the electron population of **B** is almost the same as that in S_1 at S_0-bare. This implies that the solvent assists the terminal fragments of **A** and **C** to be more polarized. At S_1/CHEX, the electron is further transferred from **A** to **C**, which ascribes to the skeletal relaxation as well as the polarization by the surrounding solvent. Consequently, these two factors stabilize the CT state at S_1/CHEX in cyclohexane.

3-2. S_1 Geometry in DMSO. In turn, we focus on the stable geometry in an aprotic polar solvent of DMSO. As pointed out in the previous subsection, the stable geometry in S_0 (i.e., S_0/DMSO) is not so affected by the surrounding solvent. However, the properties of the S_1 state are strongly affected because of a CT character in S_1. The most characteristic change is that the stable geometry of S_1 in DMSO takes a τ_2-twisted conformation (τ_2=90.0° in Table 1). This has been already pointed out by previous experiments and computations.[10−14] However, we would like to point out another essential geometrical factor of S_1/DMSO. The benzene ring of the dimethylanilino part loses its aromaticity and turns into a nonaromatic quinoid structure, as found in the case of S_1/CHEX. The linkage N^sC^4 bond becomes much shorter than that at S_0/DMSO, and the wagging angle of the dimethylamino part is close to 0°. Therefore, the resonance between the dimethylamino and the adjacent benzene ring enhances more than that in S_0. On the other hand, the linkage C^1C^α bond with a normal C−C single bond character is similar to that at S_0/DMSO, and, in addition, the dimethylanilino part is twisted against the remaining 4-cyanostyryl part. In consequence, it is possible for the dimethylanilino part to be off-resonant with the 4-cyanostyryl part. The 4-cyanostyryl group takes a planar structure substantially (τ_3=−178.3°, τ_4=1.3°). The ethylenic $C^\alpha C^{\alpha'}$ double bond is longer, and the linkage $C^{\alpha'}C^{1'}$ and $C^{4'}C^{s'}$ bonds become shorter than those at

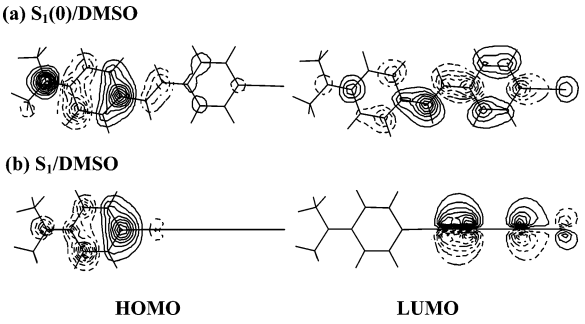

Figure 2. HOMO and LUMO (a) at $S_1(0)$/DMSO and (b) at S_1/DMSO.

S_0/DMSO, respectively. The aromatic benzene ring turns to be a nonaromatic quinoid structure. Based on these features, we can conclude that the electron-withdrawing 4-cyanostyryl group is stabilized by the delocalization over the π-conjugated fragment. Herein it is worthwhile comparing S_1/DMSO with S_1/CHEX. The loss of the aromaticity of the benzene rings is commonly found at both geometries. However, the linkage C^1C^α bond distance is very different from that at S_1/CHEX. The C^1C^α bond at S_1/DMSO is slightly shorter than a normal C−C single bond, while that at S_1/CHEX greatly increases the C═C double bond character. This difference is due to the τ_2-torsional angle: 90.0° for S_1/DMSO and 0.9° for S_1/CHEX. In other words, τ_2-torsion leads to a loss of the π-conjugation of the dimethylanilino part with the 4-cyanostyryl part, while nontwist enhances the π-conjugation between them.

Next we comment on why DCS at S_1/DMSO has a gigantic dipole moment in DMSO. We can point out the following three factors from Table 2. The S_1 dipole moment at S_0/DMSO (30.52 D) is much larger than that at the same geometry in cyclohexane (21.82 D). This means that polar DMSO polarizes DCS in S_1 more than nonpolar cyclohexane. A similar feature is also found at another perpendicularly twisted S_1/DMSO (38.27 D in DMSO, 35.93 D in cyclohexane, respectively). However, the difference of the dipole moments which depend on the solvent polarity is much smaller than that at nontwisted S_0/DMSO. This relates to another factor of the τ_2-twist. The S_1 dipole moment at S_1/DMSO (38.27 D) is much larger than that at nontwisted $S_1(0)$/DMSO (30.08 D), of which geometry is obtained by $\tau_2 = 0°$ but other parameters are fixed to those at S_1/DMSO. This means the τ_2-twist assists the charge separation between the dimethylamino group and the 4-cyanostyryl group geometrically. In Figure 2, we show the highest occupied molecular orbitals (HOMOs) and the lowest unoccupied molecular orbitals (LUMOs) at $S_1(0)$/DMSO and S_1/DMSO, respectively, which are important in describing the S_1 state. As seen in Figure 2a, especially the LUMO is delocalized over the DCS skeleton at nontwisted $S_1(0)$/DMSO. At perpendicularly twisted S_1/DMSO, on the other hand, the HOMO and the LUMO are localized over the dimethylanilino part and the 4-cyanostyryl part, respectively (see Figure 2b). In consequence, the charge separation is accomplished by the τ_2-twist. Once the charge separation is accomplished geometrically, however, the surrounding solvent serves only to stabilize the cationic and anionic fragments of the TICT geometry and is much less important to polarize DCS in S_1. This is why the difference of the dipole moments which depend on the solvent polarity is much smaller than that at S_0/DMSO. The third factor is the skeletal relaxations of both dimethylanilino and 4-cyanostyryl groups where the aromaticity of the benzene rings disappears. It is found that the τ_2-twisted quinoid geometry of S_1/DMSO has a larger dipole moment (38.27 D) than the τ_2-twisted aromatic geometry of $S_0(90)$/DMSO (36.08 D), of which geometry is obtained by $\tau_2 = 90°$ but other parameters are fixed to those at S_0/DMSO. Based on these discussions, we can ascribe a gigantic dipole moment at S_1/DMSO to solvent polarity, geometrical twist of τ_2, and the skeletal relaxation. Mulliken charges give us more detailed information on the stabilization process of the TICT formation in DMSO. Upon electronic excitation into S_1 at S_0/DMSO, the electron is transferred from the dimethylanilino part (i.e fragment **A** in Figure 1) into the benzonitrile part (fragment **C**). This means that the surrounding DMSO stabilizes both terminal fragments of the cationic **A** and the anionic **C** so as to promote the electron transfer. At τ_2-twisted S_1/DMSO, the electron is further transferred from the dimethylanilino (**A**) into the ethylenic part (**B**). In comparison with the Mulliken charge at $S_1(0)$/DMSO, it is found that the geometrical twist of τ_2 promotes additional electron transfer from the dimethylanilino into the adjacent ethylenic part.

3-3. Free Energy. To obtain more detailed information on the photochemical behavior in a solvent, we evaluated the free energies as a function of τ_2. In Figure 3, we show the free energy curves and its components of the internal energy and the electrostatic interaction in nonpolar cyclohexane. The free energy curves (denoted by S_0/CH-GM and S_1/CH-GM) in Figure 3a were obtained as a function of τ_2, while the other geometrical parameters are fixed to those at S_0/CHEX and S_1/CHEX, respectively. In other words, the aromaticity of the benzene rings is kept in the S_0/CH-GM curve, while it is lost in S_1/CH-GM. It is found that both the free energy curves have a minimum around $\tau_2 \sim 0°$ with respect to τ_2. Furthermore, S_1/CH-GM is lower than S_0/CH-GM irrespective of τ_2. This means that loss of the aromaticity and transformation into the quinoid structure are important to stabilize the S_1 state of DCS in cyclohexane. The energy decomposition gives an answer to why the skeletal-relaxed conformation without τ_2-twist is stable in nonpolar cyclohexane. As τ_2 increases, both S_0/CH-GM and S_1/CH-GM curves of the internal energy incline, which implies that the S_1 state with CT character in a nonpolar solvent prevents the τ_2-torsional motion intrinsically (see Figure 3b). However, both S_0/CH-GM and S_1/CH-GM curves of electrostatic interaction decline (see Figure 3c). In other words, the τ_2-twist promotes the electron transfer so as to reinforce the electrostatic interaction with a solvent, as pointed above. Furthermore, the S_1/CH-GM curve is lower than S_0/CH-GM irrespective of τ_2. That is, the electrostatic interaction at a skeletal relaxed form is stronger than that at an aromatic nonrelaxed form. However, reinforcement of the electrostatic interaction through τ_2-twist cannot overcome the increase of the internal energy so that the nontwisted but the skeletal-relaxed form is the most stable in S_1 with CT character.

In turn, we mention the free energy curves and their components of the internal energy and electrostatic interaction in polar DMSO. In Figure 4, we show the free energy curves of S_1 in a polar solvent of DMSO with respect to τ_2 where the other geometrical parameters are fixed to those of S_0/DMSO and S_1/DMSO (denoted by S_0/DM-GM and S_1/DM-GM, respectively). The aromaticity of the benzene rings is kept in the S_0/DM-GM curve, while it is lost in the S_1/DM-GM. With an increase of τ_2, the S_0/DM-GM curve slightly inclines the same as S_0/CH-GM. In contrast, S_1/DM-GM drastically declines so as to form the TICT state. Furthermore, S_1/DM-GM is lower than S_0/DM-GM irrespective of τ_2. This implies that the skeletal relaxation where the aromaticity of the benzene rings disappears is an essential factor for the TICT formation. The energy decomposition in Figure 4b,c gives insight into the photochemical process in polar DMSO. The internal energies increase in

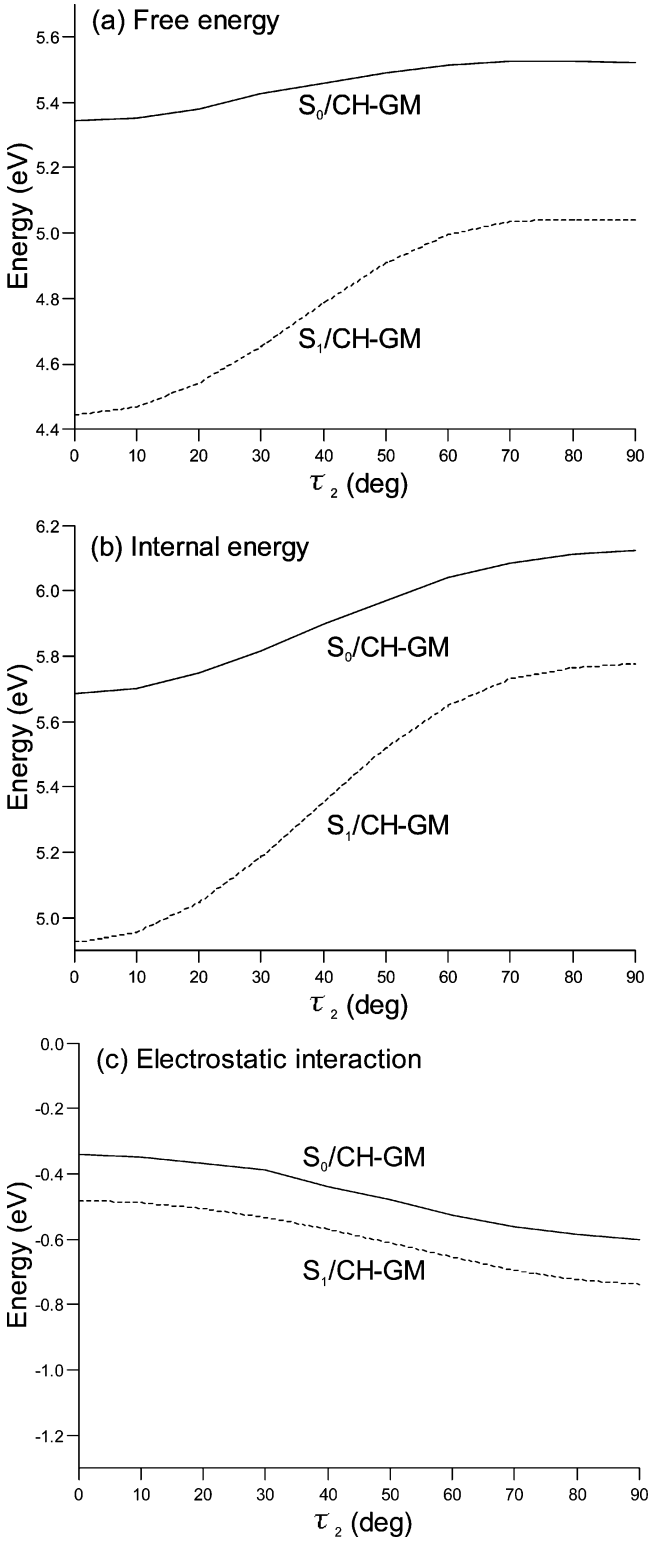

Figure 3. (a) Free energy, (b) internal energy, and (c) electrostatic interaction in cyclohexane with respect to τ_2. The other parameters are fixed to the optimized parameters at S_0/CHEX for S_0/CH-GM (in solid line) and S_1/CHEX for S_1/CH-GM (in dotted line), respectively. The free energies and internal energies are relative to the free energy in S_0 at S_0/CHEX.

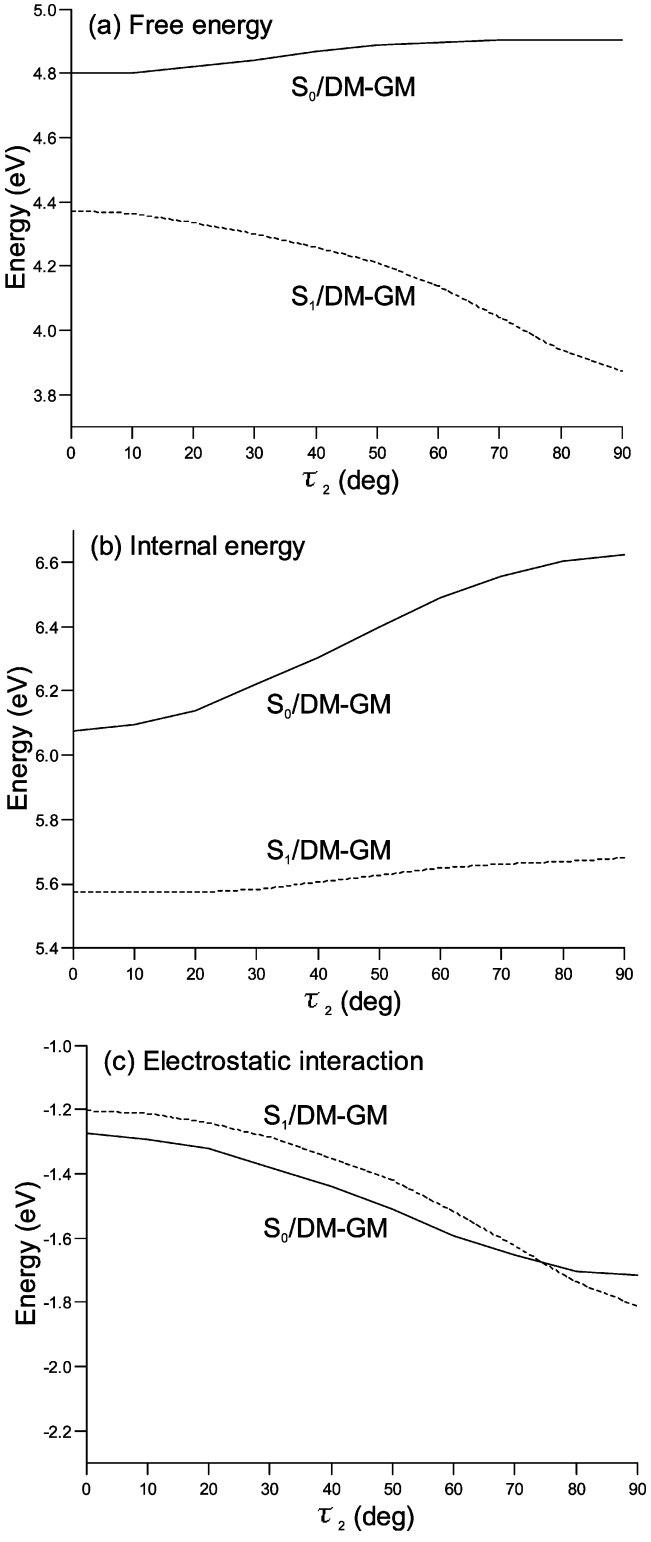

Figure 4. (a) Free energy, (b) internal energy, and (c) electrostatic interaction in DMSO with respect to τ_2. The other parameters are fixed to the optimized parameters at S_0/DMSO for S_0/DM-GM (in solid line) and S_1/DMSO for S_1/DM-GM (in dotted line), respectively. The free energies and internal energies are relative to the free energy in S_0 at S_0/DMSO.

both S_0/DM-GM and S_1/DM-GM with an increase of τ_2. In other words, τ_2-torsional motion brings about the instability of DCS itself in S_1. In more detail, however, inclination of S_1/DM-GM with respect to τ_2 is different from that of S_0/DM-GM: the former much more slowly inclines than the latter. This is ascribed to the linkage C^1C^α bond distance which governs the τ_2-torsional motion. In the former case, the C^1C^α bond is similar to a normal C−C single bond, which easily brings about the τ_2-torsional motion. In the latter case, the C^1C^α bond is shorter and slightly increases the double bond character so as to prevent the τ_2-torional motion. Regarding the electrostatic interaction, both S_1/DM-GM and S_0/DM-GM curves declines as τ_2 increases,

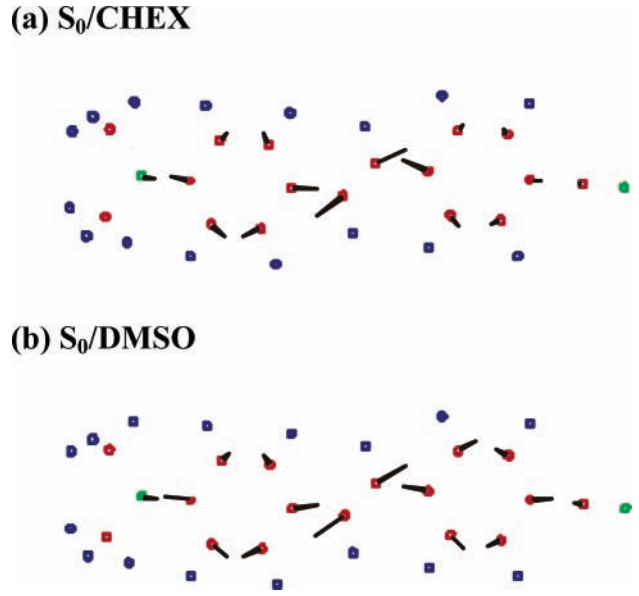

Figure 5. Force acting on each atom in S_1 at (a) S_0/CHEX and and (b) S_0/DMSO.

as found in S_1/CH-GM and S_0/CH-GM. This can be rationalized by the same reason; the τ_2-torsional motion assists the charge separation geometrically. However, the magnitude of the electrostatic interaction in a polar solvent is much larger than that in nonpolar cyclohexane (compare Figures 4c with 3c). In consequence, the softness of the τ_2-torsional motion and reinforcement of the electrostatic interaction lead to stability of the TICT conformation in a polar solvent.

3-4. Relaxation Path. In this subsection, we mention the relaxation path in a solvent on the basis of the above discussion and additional information. In nonpolar cyclohexane, the free energy curves with respect to τ_2 have a minimum around $\tau_2 \sim 0°$ (see Figure 3a). This means that electronically excited DCS directly relaxes into the most stable geometry in S_1 (S_1/CHEX) which is characterized by a nontwisted and skeletal-relaxed form. In Figure 5a, we show the S_1 force acting on each atom at S_0/CHEX where the electronic excitation takes place. Judging from the directions of the force vectors, S_0/CHEX directly changes into S_1/CHEX without the τ_2 torsion. It can be easily imagined that the reaction path in polar DMSO is different from that in nonpolar cyclohexane. This is because the τ_2 torsion in addition to the skeletal relaxation is essential to reach the most stable S_1/DMSO. So a question is which is the most realistic reaction path of the following three: (i) the skeletal relaxation takes place first and then the dimethylanilino group (i.e τ_2) is twisted, (ii) the two events of (i) take place in reverse order, and (iii) both motions take place simultaneously. As seen from Figure 5b which is substantially the same as Figure 5a, the skeletal relaxation is the most likely to take place even in DMSO. Furthermore, as deduced from the shape of S_0/DM-GM around $\tau_2 \sim 0°$ (i.e., a positive curvature around $\tau_2 = 0°$ with respect to τ_2), the τ_2-torsional motion is not so promoted upon electronic excitation into S_1. However, after the skeletal relaxation around the Franck−Condon (FC) region, the τ_2-twist takes place easily (see S_1/DM-GM in Figure 4a). In summary, only the skeletal relaxation takes place to reach the most stable S_1/CHEX in nonpolar cyclohexane. In polar DMSO, on the other hand, the skeletal relaxation first takes place to some extent, and then τ_2-torsional motion takes place to reach the most stable S_1/DMSO.

3-5. Perspective of the Model. The present model of DCS photochemistry in a solvent is based on the CASSCF calculations where the static electron correlation is included but the dynamic electron correlation effect is quite ignored. So we estimated the dynamic correlation effect by means of MRMP2 with CASSCF wave function. In Table 3, we listed the energetic corrections by MRMP2 at several important conformations. It is found that the MRMP2 energetic corrections relative to the CASSCF energies are almost constant at 1−1.3 eV, irrespective of conformations. So we think that a model based on MRMP2 calculations, which are impractical for the moment, will not change the present model by CASSCF so much.

TABLE 3: Dynamic Electron Correlation Effects on the S_1 Energies at Important Conformations[a]

geometry	CASSCF	MRMP2
	Cyclohexane	
S_0/CHEX	5.344	4.147
S_0(90)/CHEX	5.522	4.479
S_1/CHEX	4.446	3.349
S_1(90)CHEX	5.040	3.986
	DMSO	
S_0/DMSO	4.797	3.415
S_0(90)/DMSO	4.905	3.807
S_1(0)/DMSO	4.388	3.053
S_1/DMSO	3.885	2.877

[a] The S_1 energies are relative to the S_0 energy at the stable S_0 geometry in each solvent. The units are given in eV.

The essence of our present model of DCS photochemistry is to point out the importance of the skeletal relaxation as well as the dimethylanilino (i.e., τ_2) torsional motion for the CT formation in a solvent. So we estimated the effects of the skeletal relaxation and the torsional motion in a solvent in terms of the following functions of $S(\tau_2)$ and $T_i(\tau_2)$. $S(\tau_2)$ is defined in the free energy difference at τ_2 in eq 2

$$S(\tau_2) = F_1(\tau_2) - F_0(\tau_2) \tag{2}$$

where $F_1(\tau_2)$ and $F_0(\tau_2)$ are the free energies of the skeletal-relaxed conformations (i.e., S_1/CH-GM or S_1/DM-GM in Figures 3a and 4a) and the aromatic conformations (i.e., S_0/CH-GM or S_0/DM-GM) at τ_2, respectively. Considering that the free energy is decomposed into the internal energy and the electrostatic interaction, $S(\tau_2)$ can be also expressed by eq 3

$$S(\tau_2) = S^{\mathrm{int}}(\tau_2) + S^{\mathrm{ES}}(\tau_2) \tag{3}$$

where $S^{\mathrm{int}}(\tau_2)$ and $S^{\mathrm{ES}}(\tau_2)$ are the differences of the internal energies and the electrostatic interactions between the skeletal-relaxed conformations and the aromatic conformations at τ_2 (refer to Figures 3b,c and 4b,c). In other words, $S(\tau_2)$, $S^{\mathrm{int}}(\tau_2)$, and $S^{\mathrm{ES}}(\tau_2)$ are measures for how many degrees the skeletal relaxation at τ_2 affects the free energy, the internal energy, and the electrostatic interaction, respectively. $T_i(\tau_2)$ is defined by the free energy at τ_2 relative to that at nontwisted $\tau_2 = 0°$ in eq 4:

$$T_i(\tau_2) = F_i(\tau_2) - F_i(0) \quad (i=0,1) \tag{4}$$

By similar conversion of eq 2 into eq 3, we obtain eq 5 from eq 4:

$$T_i(\tau_2) = T_i^{\mathrm{int}}(\tau_2) + T_i^{\mathrm{ES}}(\tau_2) \quad (i=0,1) \tag{5}$$

$T_i(\tau_2)$, $T_i^{\mathrm{int}}(\tau_2)$, and $T_i^{\mathrm{ES}}(\tau_2)$ are measures for how many degrees the torsion up to τ_2 from 0° affects the free energy, the internal energy, and the electrostatic interaction, respectively. In Tables 4 and 5, we showed the skeletal relaxation and torsional effects

TABLE 4: Skeletal Relaxation Effect[a]

τ_2	$S(\tau_2)$	$S^{int}(\tau_2)$	$S^{ES}(\tau_2)$
	Cyclohexane		
0°	−0.899	−0.759	−0.140
90°	−0.482	−0.347	−0.135
	DMSO		
0°	−0.413	−0.484	0.071
90°	−1.018	−0.923	−0.095

[a] Units are given in eV.

TABLE 5: Torsional Effect[a]

conformation[b]	$T_i(90)$	$T_i^{int}(90)$	$T_i^{ES}(90)$
	Cyclohexane		
0	0.178	0.439	−0.261
1	0.594	0.850	−0.256
	DMSO		
0	0.105	0.547	−0.442
1	−0.500	0.108	−0.608

[a] Units are given in eV. [b] Conformations of "0" and "1" mean the aromatic benzene conformations and the nonaromatic quinoid ones, respectively.

in terms of $S(\tau_2)$ and $T_i(\tau_2)$. From Table 4, the skeletal relaxation effect on the internal energy (i.e., $S^{int}(\tau_2)$) depends on τ_2, while the electrostatic interaction (i.e., $S^{ES}(\tau_2)$) is almost independent of both cyclohexane and DMSO. In nonpolar cyclohexane, the stabilization of the internal energy (i.e., value in negative) due to the skeletal relaxation at $\tau_2 = 0°$ is larger than that at $\tau_2 = 90°$, while it is in the opposite situation in polar DMSO. Therefore, we conclude that the skeletal relaxation effect on the internal energy determines the CT geometry in a solvent. In terms of $T_i(\tau_2)$ of Table 5, we also come to the same conclusion but from a different approach. In nonpolar cyclohexane, the torsional motion stabilizes DCS through the electrostatic interaction of which is almost constant irrespective of the aromatic or skeletal-relaxed conformations. However, the torsional motion much more destabilizes DCS due to the increase of the internal energy in any cases. The destabilizations of the internal energies (i.e., value in positive) are much larger than those of the stabilization due to the electrostatic interactions. Especially, the skeletal-relaxed conformation severely impedes the torsional motion. Therefore, the nontwisted but skeletal-relaxed conformation is the most stable in cyclohexane. In polar DMSO, on the other hand, the electrostatic interaction more stabilizes DCS than in cyclohexane irrespective of the aromatic or the skeletal relaxed conformations. In addition, the internal energy at a skeletal-relaxed conformation much less impedes the torsional motion. In consequence, the torsional motion leads to a stabilization of the skeletal relaxed CT geometry in DMSO. From these discussions, we conclude that the skeletal relaxation plays an important role in the CT formation process. In other words, the CT geometry is determined by an exquisite entanglement of three factors: the skeletal relaxation, the torsional motion, and solvent polarity, as already pointed out in our previous paper on DMABN.[1]

Contrary to our model, Arzhantsev et al. very recently proposed that the DCS photochemistry is determined only by solvent relaxation.[16] That is, no geometrical twist is needed after electronic excitation into S_1, but the linear response to the surrounding solvent governs the CT formation process of DCS. If all their computational results by semiempirical calculations (refer to Figure 2 in ref 16) were reliable enough, no τ_2-twist could be right. However, we think their semiempirical calculation seems to give inconsistent conclusions about the τ_2-torsional process. As also found in our previous ab initio CASSCF calculations,[13,14] the CT state is S_1 at $\tau_2 = 0°$, but it is S_5 at $\tau_2 = 90°$ even in their semiempirical calculations. This implies that the CT state diabatically connects S_1 at $\tau_2 = 0°$ with S_5 at $\tau_2 = 90°$. However, the change of the dipole moment as a function of τ_2 seems to exhibit a little strange behavior (refer to the middle panel of Figure 2 in ref 16). That is, the dipole moments of S_1 to S_4 do not increase as an increase of τ_2 from 0°, while only the dipole moment of S_5 monotonically increases. This leads to an unrealistic interpretation that the CT state suddenly changes from S_1 into S_5 at a given τ_2 (∼30°). As far as their potential energy curves are concerned, however, it can be hardly imagined that the CT state suddenly changes from S_1 into S_5 at $\tau_2 \sim 30°$. Instead, as pointed out in the caption of Figure 2 in ref 16, the S_1 state interchanges with the S_2 state at $\tau_2 = 73°$ due to an avoided crossing. This means that the CT character in S_1 holds up to $\tau_2 \sim 70°$. In this case, however, we cannot reasonably interpret why the dipole moment S_1 decreases up to $\tau_2 \sim 70°$. As commented above and in our previous papers,[13,14] the τ_2-twist geometrically assists DCS to promote the charge separation between the dimethyanilino group and the remaining group. More strange for us to say, they did not make any comment on the skeletal relaxation effect on the CT formation. Considering our present computational result, it is hard to imagine that the two aromatic benzene rings remain unchanged after electronic excitation into S_1.

In the present paper, we emphasized the importance of the skeletal relaxation as well as the torsional motion and solvent polarity in the CT formation process. To validate our present model where the CT geometry is determined by three factors of the skeletal relaxation, torsional motion, and solvent polarity, we will do more calculations and apply our model to reinterpretation of many experimental findings as well as that by Arzhantsev et al.

4. Concluding Remarks

In this paper, we reported the CT formation of DCS in a solvent by means of CASSCF combined with the PCM method. In a nonpolar solvent, the stable CT state, in which the electron is transferred from the dimethylanilino into the 4-cyanostyryl part, takes a nontwisted conformation. However, an additional skeletal relaxation, where the aromaticity of the benzene rings disappears and the bond alternation over the whole π-conjugated system takes place, is essential for the stabilization of the CT state. In polar DMSO, the stable CT geometry takes a twisted conformation where the dimethyanilino part is highly twisted against the remaining 4-cyanostyryl part. In addition, the skeletal relaxation where the aromaticity of the benzene rings disappears is an important factor to stabilize the TICT state. The geometrical difference between the stable geometries in polar and nonpolar solvents is due to two factors: (i) the linkage bond between the dimethylanilino and the 4-cyanostyryl groups and (ii) the electrostatic interaction with a solvent. In a polar solvent, the linkage bond has a single bond character so that the torsional motion takes place easily. The electrostatic interaction is already large even at a nontwisted conformation and is reinforced through the dimethylanilino-torsional motion. In consequence, the TICT geometry is stable in a polar solvent. In a nonpolar solvent, on the other hand, the less electrostatic interaction and the hardness of the torsional motion lead to stability of a nontwisted CT conformation.

As confirmed in the present study about DCS as well as the previous one about DMABN,[1] the skeletal relaxation where the benzene ring loses its aromaticity is essential to stabilize the CT state in a solvent besides the torsional motion. So we

are now free from the unfruitful controversy of "which is right for the CT geometry, TICT model or another (for instance, PICT model)?". Instead, we should consider how much degree three factors (i.e., skeletal relaxation, torsional motion, and solvent polarity) contribute to the CT formation process.

Finally, we comment on a feature common to the photochemistry in π-conjugated molecules. The skeletal relaxation plays an important role not only in the CT formation process but also in other photoprocesses of π-conjugated molecules with aromatic benzene ring(s): the initial processes of the photoisomerization of styrene[17] and the internal conversion of diphenylacetylene[18] and phenylacetylene.[19,20] For instance, the ultrafast S_2-S_1 internal conversion of phenylacetylene is governed by effective and successive changes of the destruction and the reformation of the aromaticity of the benzene ring. We are now in progress to examine if the skeletal relaxation plays an important role not only in the benzenoid photochemistry but also in the nonbenzenoid one.

Acknowledgment. The numerical calculations were partly performed in the Computer Center of Institute for Molecular Science. This work is financially supported by Grant-in-Aid for Scientific Research from the Ministry of Education, Culture, Sports, Science and Technology.

References and Notes

(1) Amatatsu, Y. *J. Phys. Chem. A* **2005**, *109*, 7225−7235. The review on experiments and theory in therein.

(2) Rotkiewicz, K.; Grellmann, K. H.; Grabowski, Z. R. *Chem. Phys. Lett.* **1973**, *19*, 315−318

(3) Rettig, W.; Majenz, J. *Chem. Phys. Lett.* **1989**, *154*, 335−341.

(4) Gilabert, E.; Lapouyade, R.; Rullière, C. *Chem. Phys. Lett.* **1991**, *185*, 82−87.

(5) Lapouyade, R.; Czechka, K.; Majenz, W.; Rettig, W.; Gilabert, E.; Rullière, C. *J. Phys. Chem.* **1992**, *96*, 9643−9650.

(6) Rettig, W.; Majeiz, W.; Herter, R.; Létard, J.-F.; Lapouyade, R. *Pure Appl. Chem.* **1993**, *65*, 1699−1704.

(7) Rettig, W.; Gilabert, E.; Rullière, C. *Chem. Phys. Lett.* **1994**, *229*, 127−133.

(8) Létard, J.-F.; Lapouyade, R.; Rettig, W. *Chem. Phys. Lett.* **1994**, *229*, 209−216.

(9) König, N. E.; Kühne, T.; Schwarzer, D.; Vöhringer, P.; Schroeder, J. *Chem. Phys. Lett.* **1996**, *253*, 69−76.

(10) Abraham, E.; Oberlé, J.; Jonusauskas, G.; Lapouyade, R.; Rullière, C. *Chem. Phys.* **1997**, *214*, 409−423.

(11) Abraham, E.; Oberlé, J.; Jonusauskas, G.; Lapouyade, R.; Rullière, C. *J. Photochem. Photobiol. A* **1997**, *105*, 101−107.

(12) Pines, D.; Pines, E.; Rettig W. *J. Phys. Chem. A* **2003**, *107*, 236−242.

(13) Amatatsu, Y. *Theor. Chem. Acc.* **2000**, *103*, 445−450.

(14) Amatatsu, Y. *Chem. Phys.* **2001**, *274*, 87−98.

(15) Schmidt, M. W.; Baldridge, K. K.; Boatz, J. A.; Elbert, S. T.; Gordon, M. S.; Jensen, J. H.; Koseki, S.; Matsunaga, N.; Nguyen, K. A.; Su S. J.; Windus, T. L.; Dupuis, M.; Montgomery, J. A., Jr. *J. Comput. Chem.* **1993**, *14*, 1347−1363.

(16) Arzhantsev, S.; Zachariasse, K. A.; Maroncelli, M. *J. Phys. Chem. A* **2006,** *110*, 3454−3470.

(17) Amatatsu, Y. *J. Comput. Chem.* **2002**, *23*, 950−956.

(18) Amatatsu, Y.; Hasebe, Y. *J. Phys. Chem. A* **2003**, *107*, 11169−11173.

(19) Amatatsu, Y.; Hosokawa, M. *J. Phys. Chem. A* **2004**, *108*, 10238−10244.

(20) Amatatsu, Y. *J. Phys. Chem. A* **2006**, *110*, 4479−4486.